Curr Genet (2015) 61:555–566
DOI 10.1007/s00294-015-0476-z

RESEARCH ARTICLE

Isolation and functional analysis of the pathogenicity-related gene *VdPR3* from *Verticillium dahliae* on cotton

Ya-Lin Zhang · Zhi-Fang Li · Zi-Li Feng · Hong-Jie Feng · Li-Hong Zhao · Yong-Qiang Shi · Xiao-Ping Hu · He-Qin Zhu

Received: 23 November 2014 / Revised: 29 December 2014 / Accepted: 25 January 2015 / Published online: 5 February 2015

Abstract The fungal plant pathogen *Verticillium dahliae* is the causal agent of vascular wilt, a disease that can seriously diminish cotton fiber yield. The pathogenicity mechanism and the identity of the genes that interact with cotton during the infection process still remain unclear. In this study, we investigated the low-pathogenic, non-microsclerotium-producing mutant vdpr3 obtained in a previous study from the screening of a T-DNA insertional library of the highly virulent isolate Vd080; the pathogenicity-related gene (*VdPR3*) in wild-type strain Vd080 was cloned. Knockout mutants (ΔVdPR3) showed lower mycelium growth and obvious reduction in sporulation ability without microsclerotium formation. An evaluation of carbon utilization in mutants and wild-type isolate Vd080 demonstrated that mutants-lacking *VdPR3* exhibited decreased cellulase and amylase activities, which was restored in the complementary mutants (ΔVdPR3-C) to levels similar to those of Vd080. ΔVdPR3 postponed infectious events in cotton and showed a significant reduction in pathogenicity. Reintroduction of a functional *VdPR3* copy into ΔVdPR3-C restored the ability to infect cotton plants. These results suggest that *VdPR3* is a multifunctional gene involved in growth development, extracellular enzyme activity, and virulence of *V. dahliae* on cotton.

Keywords *Verticillium dahliae* · *VdPR3* · Biological characteristics · Virulence · Extracellular enzyme

Introduction

As the primary natural fiber crop, cotton (*Gossypium hirsutum* L.) is of great importance to the global agricultural economy. Verticillium wilt disease, caused by the phytopathogenic fungus *Verticillium dahliae* Kleb, is a major threat to cotton production, especially in China (Xia et al. 1998; James 2002). This widespread and destructive soil-borne fungal pathogen has more than 200 plant hosts besides cotton and causes enormous economic losses (Pegg and Brady 2002; Fradin and Thomma 2006; Klosterman et al. 2009). Microsclerotia are stable melanized dormant structures of *V. dahliae* required for successive infection; they can endure multiple adversities and survive for more than 10 years in plant debris and soil (Schnathorst 1981). After germination of microsclerotia or conidia around roots, the infectious hyphae penetrate root tips, root wounds, or lateral roots. The hyphae then spread through cortical and vascular tissues to disrupt water transport and cause characteristic plant wilt symptoms accompanied by vascular discoloration (Tsror and Levin 2003; Vallad and Subbarao 2008).

To help elucidate the complex virulent signaling pathways in *V. dahliae* and to promote the development of effective targeted control strategies, several technological methods, including both forward and reverse genetics measures, have been used for functional analysis of pathogenicity-related

Communicated by Z. Zhang.

Ya-Lin Zhang and Zhi-Fang Li contributed equally to this work.

Y.-L. Zhang · Z.-F. Li · Z.-L. Feng · H.-J. Feng · L.-H. Zhao · Y.-Q. Shi · H.-Q. Zhu (✉)
State Key Laboratory of Cotton Biology, Institute of Cotton Research of Chinese Academy of Agricultural Sciences, Anyang 455000, Henan, China
e-mail: heqinanyang@163.com

X.-P. Hu (✉)
State Key Laboratory of Crop Stress Biology for Arid Areas, College of Plant Protection, Northwest A&F University, Yangling 712100, Shaanxi, China
e-mail: xphu@nwsuaf.edu.cn

genes. One such approach involves the screening of an expressed sequence tag (EST) library. For example, two cDNA libraries constructed from different inducing cultures of *V. dahliae* have provided useful model systems for pathogenesis and microsclerotium development analysis (Neumann and Dobinson 2003). Based on the results of EST library screening, *VdNEP* (necrosis- and ethylene-inducing protein) has been shown to have specific importance for vascular wilt symptoms of cotton leaves and to be critical for virulence (Wang et al. 2004). Another important strategy is exploration of the function of crucial genes or families involved in virulence pathways. For instance, a functional analysis was conducted on the *VdNLP* (necrosis- and ethylene-inducing-like protein) family comprising nine members in *V. dahliae*. Among these genes, *VdNLP*1 and *VdNLP*2 were found to induce necrotic lesions and trigger defense responses in several plant species (Zhou et al. 2012a). The virulence-inducing function of *NLP* genes varies among plant hosts. In two studies, targeted deletion mutants significantly compromised virulence on tomato as well as *Arabidopsis* plants, but did not affect the infectious ability of *V. dahliae* against cotton (Santhanam et al. 2013; Zhou et al. 2012b). *VGB* (G protein β subunit) has been demonstrated to play an important role in virulence, hormone production, and the developmental signaling pathway in *V. dahliae* (Tzima et al. 2012). Multi-faceted *VDH1* (class-II hydrophobin) is critical for microsclerotium production and nutrient availability, but is not needed for disease development in tomato (Klimes and Dobinson 2006; Klimes et al. 2008). *Verticillium dahliae* mutants-lacking *VMK1* (a mitogen-activated protein kinase gene) have been observed to significantly reduce microsclerotium formation and decreased pathogenicity on diverse hosts (Rauyaree et al. 2005). The sucrose non-fermenting one gene (*VdSNF1*), which regulates catabolic repression, is required for virulence and expression of genes involved in cell-wall degradation (Tzima et al. 2011). A third useful approach is the screening of T-DNA insertional mutant libraries and the exploitation of pathogenicity-related candidates. Large-scale pathogenicity tests on lettuce have facilitated the selection of mutants with distinctly lower virulence for targeted gene function analysis (Maruthachalam et al. 2011). In one study, the Vdgarp1 mutant obtained from a *V. dahliae* V952 insertional library showed vigorous mycelium growth with a significant delay in melanized microsclerotial formation and weak virulence to cotton seedlings (Gao et al. 2010). Finally, comparative genomic analyses have revealed the pathogenicity-specific sequence of *V. dahliae*. Compared on the genomic level with other pathogenic fungi, the glucosyltransferase homolog VDAG_02071 specific to *V. dahliae* was selected and identified as one of the main virulence factors. Through the use of comparative genomics between low- and high-virulence isolates, the specific secreted protein gene (*VdSSP1*) of a highly virulent defoliating *V. dahliae* pathotype associated with plant cell-wall degradation and virulence to cotton was located in the specific sequence SCF73 (Liu et al. 2013).

In a previous study, we constructed an *Agrobacterium tumefaciens*-mediated transformation (ATMT) insertional mutant library of highly virulent *V. dahliae* Vd080 that included over 2,000 mutants with diverse biological characteristics (Zhou et al. 2012a). We screened 800 mutants for changes in virulence through two rounds of testing. Compared with the wild-type isolate Vd080, vdpr3 showed significantly lower virulence against cotton seedlings and produced no microsclerotia. In this study, we cloned the pathogenicity-related gene *VdPR3* by thermal asymmetric interlaced PCR (TAIL-PCR). We evaluated the role of *VdPR3* in the virulence of the highly virulent isolate Vd080 on Verticillium wilt susceptible cotton variety Jimian11. Functions associated with microsclerotium development and extracellular enzyme activity were also investigated.

Materials and methods

Fungal isolates, media, cotton plants, and culture conditions

In this study, we used the virulent defoliating *V. dahliae* isolate Vd080 from cotton collected in Xinji, Hebei, China. Vd080 and its transformants were single-spore isolated and stored in 20 % glycerol at −80 °C. The low-pathogenic mutant vdpr3 was selected from the T-DNA insertional library of *V. dahliae* strain Vd080. Potato dextrose agar (PDA) medium was used for isolate reactivation, amplification, and observation of biological characteristics. Conidia were prepared for pathogenicity assays, and the homogeneous inoculum was cultured in liquid Czapek-Dox medium (30 g/L Sucrose, 2 g/L $NaNO_3$, 0.5 g/L $MgSO_4{\cdot}7H_2O$, 0.5 g/L KCl, 0.02 g/L $FeSO_4{\cdot}7H_2O$, and 1 g/L K_2HPO_4) at 25 °C in a shaker incubator at 150 rpm. *Escherichia coli* trans1-α and *Agrobacterium tumefaciens* strain AGL-1 were routinely grown in Luria–Bertani medium (Sambrook et al. 2001) with appropriate antibiotics and incubated at 37 and 28 °C, respectively. Transformations of bacterial plasmid DNA were performed using a standard chemical protocol (Sambrook and Russell 2001). Plants of the cotton cultivar Jimian 11, a highly Verticillium wilt susceptible variety, were cultivated in a standard greenhouse at 25–30 °C under a 16-h/8-h light–dark photoperiod.

Isolation of *VdPR3*, gene cloning, and analysis

Bidirectional flanking sequences of the T-DNA insert in the vdpr3 mutant were identified by TAIL-PCR. Right ($R\text{-}SP_1$, $R\text{-}SP_2$, and $R\text{-}SP_3$) and left ($L\text{-}SP_1$, $L\text{-}SP_2$, and $L\text{-}SP_3$)

Table 1 Primers used in this study

Primer names	Primer sequence (5'-3')
VdPR3 cloing	
ORF-F	ATGCAGCTTCCAGGGCAAG
ORF-R	TTAAACGATTTTGGACGCCC
Construct *VdPR3* knockout vector	
HPH-F	TTGAAGGAGCATTTTTGGGC
HPH-R	TTATCTTTGCGAACCCAGGG
P1	GCCTTGTGAATGCTGTGCGT
P3	GCCCAAAAATGCTCCTTCAACGCAACTTGTCCTCCCAAGC
P4	CCCTGGGTTCGCAAAGATAA CGGAGACGAGCGAACGAAGA
P6	AACGGCTCGAACGGCTCAAT
P2	GGGGACAAGTTTGTACAAAAAAGCAGGCTCTTCGTTGGACTCGGGGGAG
P5	GGGGACCACTTTGTACAAGAAAGCTGGGTCCAGACAGGCGCTCGGAATA
Test-F	CAGGGCAAGACTGCCCAC
Test-R	CCCAGCCTGTCTAAACCCTT
Construct *VdPR3* complementary vector	
COM-F	GAATTCTGGCCAGCTGATGTCGTGAT
COM-R	CTTAAGCTGCCTACCTAGCGACCACA
GFP-F	ATGCCGTGAGTGATCCCGGCGGC
GFP-R	ATGGTGAGCAAGGGCGAGGAGCT
VdPR3 transcriptional level testing	
RT-F	AGCTTCCAGGGCAAGACTGC
RT-R	CTCCATCTCCCTTCCGCCTG
Vdβt-F	AACAACAGTCCGATGGATAATTC
Vdβt-R	GTACCGGGCTCGAGATCG

Underlined regions are the complementary sequence to HPH-F/R and P3/P4, respectively; wavy lines refer to attB1 and attB2 for the Gateway BP reaction, and dashed lines indicate restriction enzyme recognition sites

border primers specific to the binary vector pCTHyg were used as previously described (Liu et al. 2015). Four arbitrary degenerate primers were designed according to previous research (Liu et al. 1995). TAIL-PCR amplifications were performed in a PCR thermocycler (EDC-810; Eastwin, Beijing, China) using a genome walking kit (Takara, Dalian, China). The tertiary PCR products obtained from both sides of the T-DNA were cloned and sequenced by Genewiz Corporation, Nanjing, China. The specific primer, either R-SP_3 or L-SP_3, was used as the sequencing primer. The sequencing fragments were aligned using the T-DNA sequence and the VdLs.17 genome database to ascertain the insertion site and disrupted gene of wild-type isolate Vd080. Using the obtained information, the complete open reading frame (ORF) of the pathogenicity-related gene *VdPR3* was successfully cloned from Vd080 using ORF-F and ORF-R specific primers under reaction conditions of 30 cycles of 94 °C for 1 min, 60 °C for 1 min, and 72 °C for 45 s. Similarity analysis and homolog function prediction were performed using the BLAST program (Altschul et al. 1997).

Vector construction and fungal transformation

A series of primers was designed based on *VdPR3*, 2,000 bp upstream, 2,000 bp downstream, and skeleton vector sequences (Table 1). Generation of a knockout-infused fragment consisted of three steps: specific amplification, fusion PCR, and nested amplification. Primer pairs P1/P3 and P4/P6 were used to, respectively, amplify a 1.1 kb upstream fragment (UP) and a 1.2 kb downstream fragment (DOWN) from Vd080 genomic DNA. A ~1.8 kb hygromycin cassette (HPH) was amplified from the pCTHyg vector using HPH-F and HPH-R primers. More specifically, the reverse complementary adaptors of HPH-F and HPH-R were added to the primers P3 and P4, respectively. Making use of specific recognition of these adaptors, a fusion PCR was conducted to connect UP, HPH, and DOWN amplicons in a ratio of 1:3:1 (Yu et al. 2004). A nested PCR was then carried out with the fusion fragment as the template using primers P2 and P5, which contained Gateway BP reaction adaptors. The final amplicon was cloned into the *Agrobacterium* binary pGKO2-gateway vector by a BP recombinant reaction (Invitrogen, Carlsbad, CA, USA) to yield pGKO-VdPR3 (Khang et al. 2005). The pGKO2 vector carried a lethal gene, herpes simplex virus thymidine kinase (*HSVtk*), as a negative selection marker against ectopic transformants.

To generate the *VdPR3* complementary vector, we carried out restriction enzyme digestion and ligation. A ~2.5 kb fragment including 1.2 kb upstream, *VdPR3* (762 bp), and 500 bp downstream regions was amplified from the genomic DNA of strain Vd080 using primers COM-F and COM-R, which contained *EcoRI* and *AF1II* recognition site adaptors, respectively. The 2.5 kb fragment was cloned into the binary vector pSULPH-gfp carrying a chlorimuron-ethy1 resistance gene cassette and the green fluorescent protein (GFP) gene (Zhou et al. 2009). The positive clones were named as pSUL-VdPR3.

ATMT of *V. dahliae* Vd080 with pGKO-VdPR3 was performed as described previously (Mullins et al. 2001) with some modifications. A co-culture of *V. dahliae* spores (5×10^6 CFU/mL) and *A. tumefaciens* cells (OD = 0.3–0.4) carrying knockout or complementary vectors was incubated on Hybond membranes (Amersham Pharmacia) at 25 °C for 48 h. The selection medium contained 50 μg/mL spectinomycin and 50 μg/mL cefotaxime to inhibit the growth of *A. tumefaciens* cells. To obtain the *VdPR3* deletion mutants from wild isolate Vd080, the selection medium was additionally supplemented with 50 μg/mL hygromycin and 50 μmol/L 5-fluoro-2-deoxyuridine (F2dU) (Sigma) and incubated until colonies appeared. The nucleoside analog F2dU excluded ectopic transformants (Khang et al. 2005).

For complementation experiments, the complementary vector pSUL-VdPR3 was introduced into the T-DNA insertion mutant vdpr3. Positive transformants were screened on PDA medium supplemented with 50 μg/mL chlorimuron-ethy1. Both the knockout and complementary mutants were purified as single-spore isolates.

Molecular identification of *VdPR3* disruption or complementary mutants

Initial screening of transformants for the desired disruption and reintroduction of a functional *VdPR3* copy into the T-DNA insertional mutant vdpr3 was carried out by PCR using the tested primers (Table 1). Primers HPH-F/R were designed to determine the replacement between the hygromycin-resistance cassette and the *VdPR3* gene in the disruption mutants. Successful ΔVdPR3 knockout recombinants tested positive for the HPH-targeted fragment without *VdPR3*. Positive complementary mutants had chlorimuron-ethy1 resistance, which was identified with COM-F/R. To examine the transcription profile of *VdPR3* in both mutants, transcription levels of the target gene based on RT-F/R primers were quantified relative to the constitutively expressed β-tubulin gene amplified with primers Vdβt-F and Vdβt-R. PCR cycling consisted of an initial denaturation step of 94 °C for 2 min, followed by 40 cycles of 94 °C for 10 s and 60 °C for 30 s.

Phenotypic characterization

Mutants derived from Vd080 were characterized for their developmental and morphological characteristics. To

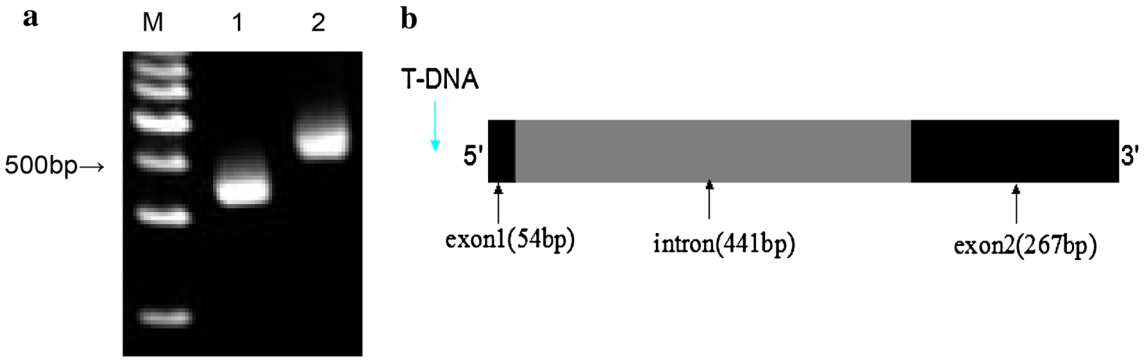

Fig. 1 Cloning and gene structure of *VdPR3*. **a** Electrophoretogram of the *VdPR3* cloning process. *M*: marker; *lane 1*: ORF of *VdPR3* cloned from cDNA of Vd080; *lane 2*: *VdPR3* cloned from the genome of Vd080. **b** Schematic diagram showing the position of the T-DNA insertion in the vdpr3 mutant and the structure of the *VdPR3* gene

ensure uniform amounts of inoculum, 5 μL conidial suspensions (1×10^7 CFU/mL) of each strain were inoculated on PDA medium containing no antibiotics. Colony diameters were recorded at 3, 5, 7, 9, and 11 days post-inoculation (dpi), and fungal growth phenotypes were observed. Green fluorescence of positive complemented colonies was visualized using a compound microscope equipped with a GFP filter.

To evaluate the conidium production ability of different mutants, 5 μL fresh spore suspensions (1×10^7 CFU/mL) of each strain were inoculated into 40 mL of liquid Czapek-Dox medium at 25 °C in a shaker incubator at 150 rpm. Wild-type strain Vd080 was used as a comparison. Conical bottles were shaken gently, and the number of conidia in 10 μL spore suspensions was counted in a hematocytometer.

To analyze carbon source utilization of the mutants, skim milk powder (18 g/L), cellulose (5 g/L), and starch (1 g/L) were individually added to Czapek-Dox medium lacking sucrose. 5 μL conidial suspensions (1×10^7 CFU/mL) of each strain were then inoculated onto plates containing one of the different carbon sources, followed by incubation at 25 °C in the dark. To determine protease, cellulase, and amylase activities, colony diameters were recorded at one day intervals. The experiment was repeated twice ($n = 3$).

Pathogenicity assays

The cotton cultivar Jimian 11, which is highly susceptible to Verticillium wilt, was used to evaluate the effect of *V. dahliae* wild-type strain Vd080 and its mutants on virulence. The experiment was conducted in a greenhouse at 25–30 °C under a 16-h/8-h light–dark photoperiod. Eight to ten cotton seedlings were inoculated per treatment, with three treatments carried out per isolate. The inoculation concentration was uniformly adjusted to 1×10^7 CFU/mL. The infection assay procedure is detailed in our previous report (Zhu et al. 2013). Symptom development was observed from 7 to 26 days after inoculation. Disease severity was rated according to a disease index (DI) based on five-scale categorization of Verticillium wilt disease on cotton seedlings (Zhu et al. 2013). The infection assay was repeated three times for each mutant.

Results

VdPR3 isolation and sequence analysis

In a previous study (Liu et al. 2015), the vdpr3 mutant had been confirmed by DNA blot analysis to have a single copy of the T-DNA insert. We carried out TAIL-PCR using primers specific for both T-DNA flanking regions. The functional gene disrupted by T-DNA in vdpr3 was found to be highly similar to VDAG_09942 from the VdLs.17 reference genome database, with the T-DNA insert located 95 bp upstream of VDAG_09942 (*VdPR3*). Further analysis of gene structure revealed that the full-length sequence of *VdPR3* was 762 bp long and comprised two exons (54 and 267 bp) and one intron (441 bp). A schematic diagram of *VdPR3* gene structure showing the position of the T-DNA insertion is given in Fig. 1. The ORF of *VdPR3* was predicted to encode a protein of 106 amino acids that displayed 99 % identity with VDAG_09942. Neither the nucleotide nor the amino acid sequence shared more than 80 % similarity with any other annotated gene in the NCBI non-redundant protein sequence database.

Disruption and complementation of the *VdPR3* gene in *V. dahliae*

A *VdPR3*-disrupted vector was generated by replacing the complete *VdPR3* gene with a hygromycin-resistance

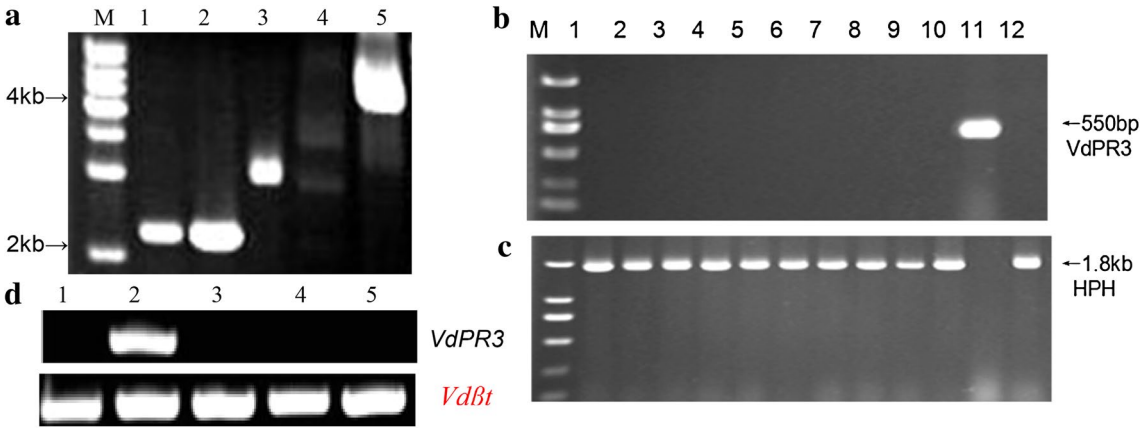

Fig. 2 *VdPR3* knockout vector construction and molecular identification of positively disrupted ΔVdPR3 mutants. **a** Electrophoretic image from construction of the gene-knockout plasmid of pGKO-VdPR3. *Lane 1*: upstream fragment; *lane 2*: downstream fragment; *lane 3*: HPH cassette; *lane 4*: fusion fragment; *lane 5*: homologous recombination fragment. **b** Amplification of the *VdPR3* gene. *Lanes 1–10*: ΔVdPR3 mutant*; lane 11*: Vd080; *lane 12*: knockout vector. **c** Amplification of the HPH gene. *Lanes 1–10*: ΔVdPR3 mutant*; lane 11*: Vd080; *lane 12*: knockout vector. **d** RT-PCR was used to detect *VdPR3* expression levels*, Vdβt* was used as a control. *Lane 1*: vdpr3; *lane 2*: Vd080; *lanes 3–5*: ΔVdPR3 mutant

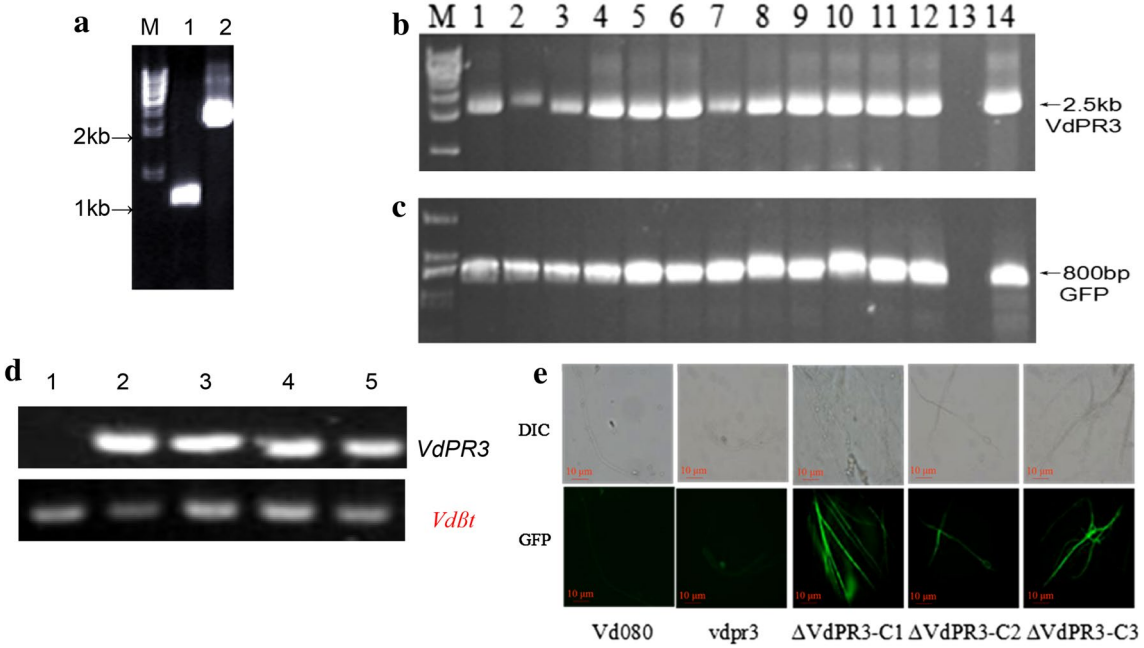

Fig. 3 Construction of the *VdPR3* complementary vector and screening of mutants. **a** Electrophoretic image from the construction of the gene-complementary plasmid of pSUL-VdPR3. *Lane 1*: GFP fragment; *lane 2*: VdPR3 complementary fragment. **b** Amplification of *VdPR3*. *Lanes 1–12*: complementary mutant*; lane 13*: vdpr3; *lane 14*: complementary vector. **c** Amplification of GFP. *Lanes 1–12*: complementary mutant*; lane 13*: vdpr3; *lane 14*: complementary vector. **d** RT-PCR was used to confirm the expression of *VdPR3, Vdβt* was used as a control. *Lane 1*: vdpr3; *lane 2*: Vd080; *lanes 3–5*: complementary vector. **e** Observation of green fluorescence under visible-light and fluorescence microscopes. *Bar* 10 μm

cassette. Approximately 1.1 kb upstream and 1.2 kb downstream regions of *VdPR3* were, respectively, amplified with primers P1/P3 and P4/P6 from wild-type isolate Vd080, and a ~1.8 kb fragment of the hygromycin cassette was excised from the pCTHyg vector. A ~4.1 kb fusion fragment made up of UP, HPH, and DOWN was obtained by successive PCR fusions that relied on reverse complementary adaptor recognition. A nested PCR with

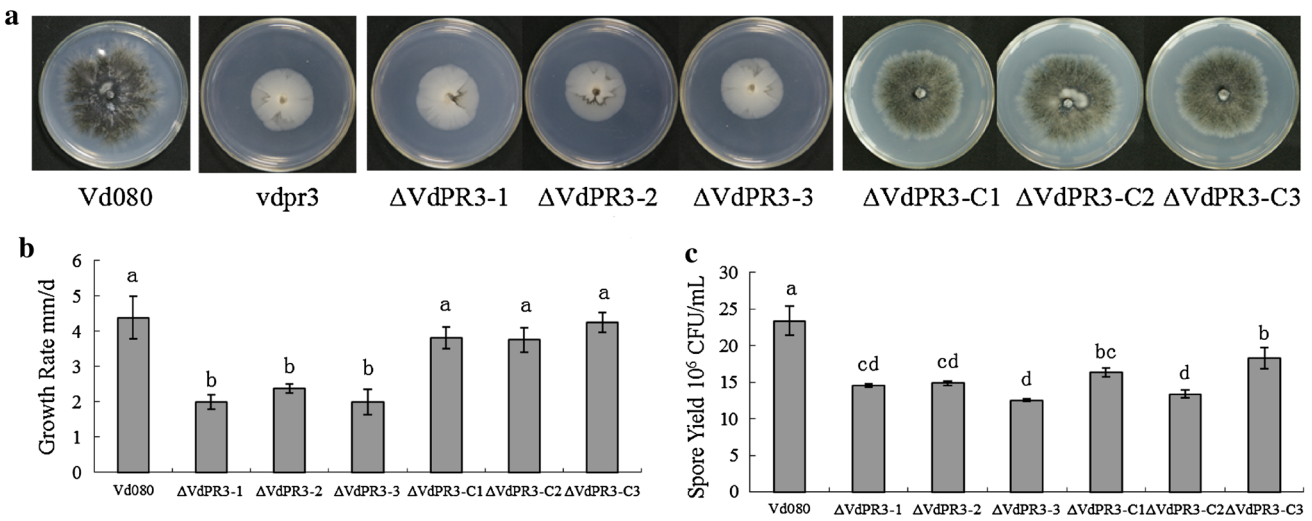

Fig. 4 Phenotypic characterization of the wild-type strain and mutants. **a** Colony morphology of the wild-type strain and mutants on potato dextrose agar at 11 dpi. **b** Radial growth rates of isolates. **c** Spore yield of mutants. Means and standard errors were calculated from at least three independent experiments, with a significant difference of $P < 0.05$ between strains

P2/P5 primers was conducted to amplify the targeted UP–HPH–DOWN fragment with attB adaptors on both sides (Fig. 2a). A pGKO-VdPR3 vector was constructed by BP recombination between a pGKO2-Gateway binary vector and the UP–HPH–DOWN fusion fragment. *Agrobacterium tumefaciens* carrying pGKO-VdPR3 was introduced into wild-type strain Vd080. *HSVtk* located on the pGKO-VdPR3 vector acted as a negative selection marker against ectopic transformants. PCR analysis revealed a homologous recombination event at the *VdPR3* locus in 10 of 35 positive knockout mutants of *V. dahliae* Vd080, corresponding to a 28.6 % positive transformant efficiency rate. In contrast to wild-type Vd080, an HPH fragment was amplified without *VdPR3* detection in ΔVdPR3 mutants (Fig. 2b, c). Three of the mutants (ΔVdPR3-1, ΔVdPR3-2, and ΔVdPR3-3) were randomly selected for further functional analysis of *VdPR3*. The absence of the *VdPR3* transcript in these three mutants was confirmed by RT-PCR analysis (Fig. 2d).

For complementation, a complete functional copy of *VdPR3* including the native promoter and terminator elements was successfully integrated into the binary vector pSULPH-gfp (Fig. 3a). *Agrobacterium tumefaciens* carrying the complementary vector was transferred into the T-DNA inserted mutant vdpr3. Finally, 31 chlorimuronethy1 resistant transformants were obtained, of which 12 were randomly selected for molecular identification. PCR amplification of all 12 transformants using COM-F/R and GFP-F/R primers yielded expected products of the ~2.5 kb complete *VdPR3* gene and ~800 bp GFP, respectively, (Fig. 3b, c). The expression profile of *VdPR3* in complementary mutants (ΔVdPR3-C1, ΔVdPR3-C2, and ΔVdPR3-C3) was examined using RT-F/R primers, with the β-tubulin gene (*Vdβt*) used as an internal control. Fortunately, wild-type Vd080 and the ΔVdPR3-C mutants exhibited similar *VdPR3* transcription levels (Fig. 3d). Under a fluorescence microscope, however, mycelia of all ΔVdPR3-C isolates displayed significant green fluorescence that differed from that of Vd080 and vdpr3 (Fig. 3e).

VdPR3 participation in microsclerotium development, mycelial growth, and spore production

To explore the role of *VdPR3* in *V. dahliae* growth and development, the above-mentioned three gene-disrupted mutants and the three complementary mutants were compared with Vd080. On PDA medium, the colony morphology of Vd080 and the complementary mutants was very similar, with abundant microsclerotium production and a high concentration of melanin. The deletion mutants had white mycelia without microsclerotia (Fig. 4a). The importance of *VdPR3* in microsclerotium production was thus demonstrated. Radial growth of the deletion mutant ΔVdPR3 was always slower than that of Vd080, with the corresponding growth rate of ΔVdPR3 decreased significantly. The ΔVdPR3-C complementary mutants restored the growth rate to an average of 3.94 mm/d, nearly as high as, and not significantly different from, that of Vd080 (4.38 mm/d) (Fig. 4b). Compared with the spore production of wild-type Vd080 (23.38×10^6 CFU/mL), that of the knockout mutants was significantly reduced with an average biomass of 13.99×10^6 CFU/mL. This reduced sporulation suggests that *VdPR3* is involved in the regulation of spore production in *V. dahliae*, but it was not recovered

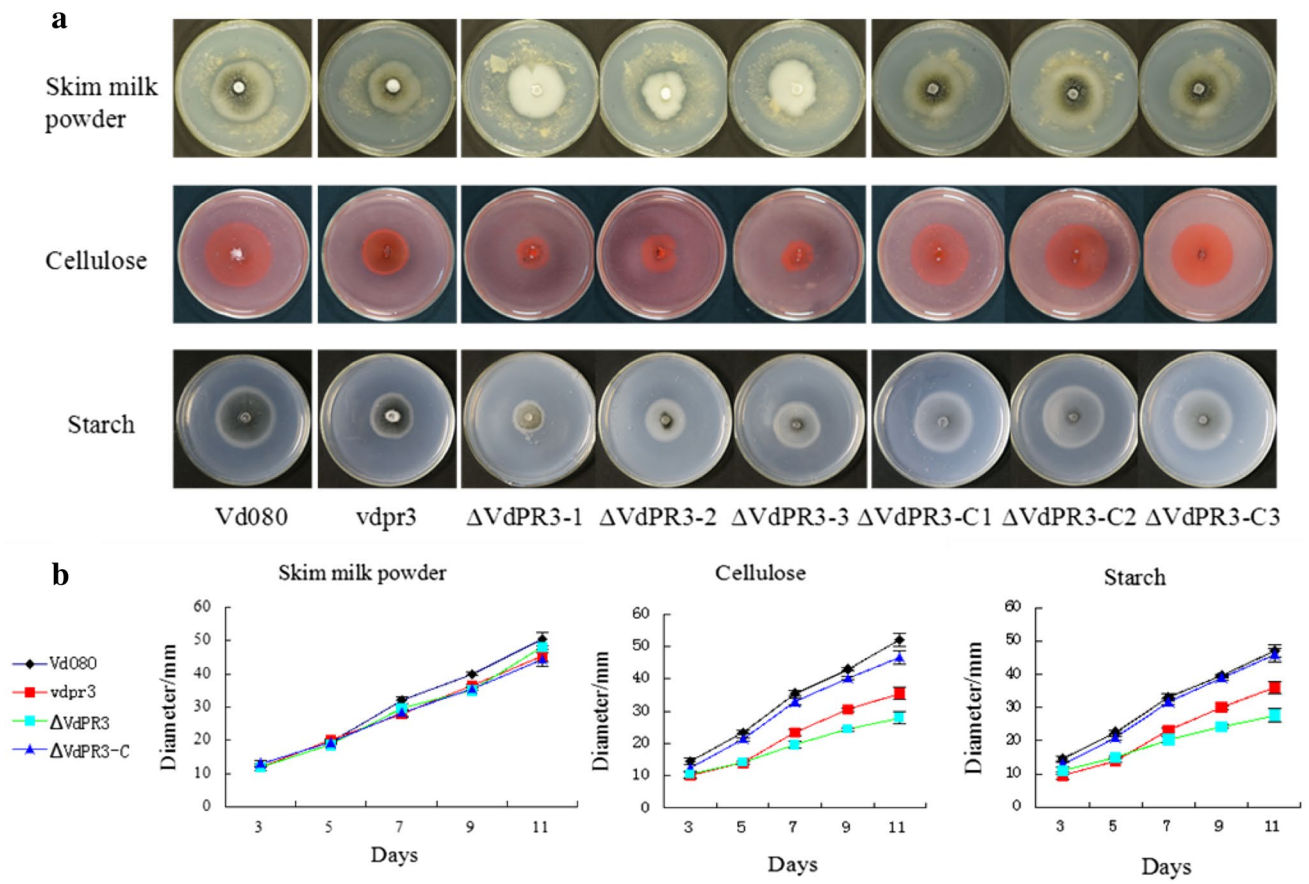

Fig. 5 Cultural characteristics and growth rates of isolates on different carbon source media. **a** Phenotypes of mutants and Vd080. **b** Radial growth rates of isolates. Means and standard errors were calculated from at least three independent experiments, with a significant difference of $P < 0.05$ between strains

in the complemented strains, especially in ΔVdPR3-C2 (13.37×10^6 CFU/mL) (Fig. 4c).

Cellulase and amylase activity of *VdPR3*

To investigate the ability of *VdPR3* to degrade different carbon sources, we compared radial growth rates of wild-type strain Vd080 and mutants on skim milk, cellulose, and starch. All strains grew at similar rates on skim milk powder, demonstrating that the product of *VdPR3* did not contribute to protease ability. Two different outcomes were observed on cellulose and starch media. Similar to the vdpr3 mutant, the ΔVdPR3 knockout mutants grew on cellulose medium at a minimum rate of 2.19 ± 0.38 mm/d without an obvious transparent circle; this rate was significantly lower than in the wild-type strain Vd080 (4.69 ± 0.31 mm/d). Gene complementation restored the cellulase activity of the isolates. These results indicate that *VdPR3* is involved in cellulose utilization. Compared with the wild-type strain Vd080, the growth rate of the *VdPR3* knockout mutants decreased by 46 % on a starch-Czapek medium. In other words, the isolates lacking the *VdPR3* gene had reduced starch decomposition ability. Complementation of the mutants with a functional *VdPR3* copy restored growth on starch to wild-type levels (Fig. 5).

Role of *VdPR3* in virulence

To further evaluate the role of *VdPR3* in pathogenicity, we tested and analyzed the pathogenic ability of different mutants and wild type isolate Vd080 on cotton seedlings. After 7 days of infection, cotton plants inoculated with wild-type Vd080 presented severe symptoms of chlorosis and stunting in some leaves. In contrast, the ΔVdPR3 knockout mutants caused no visible symptoms in cotton until 13 dpi. At 26 dpi, most cotton seedlings inoculated with Vd080 were dead, and the DI value reached 55.62 ± 4.0. In contrast, the ΔVdPR3 deletion mutants showed weakened ability to infect cotton plants, which showed only slight Verticillium wilt symptoms. Compared with the wild type, the DI values of ΔVdPR3 were remarkably reduced ($P < 0.01$), ranging from 20.67 ± 3.2

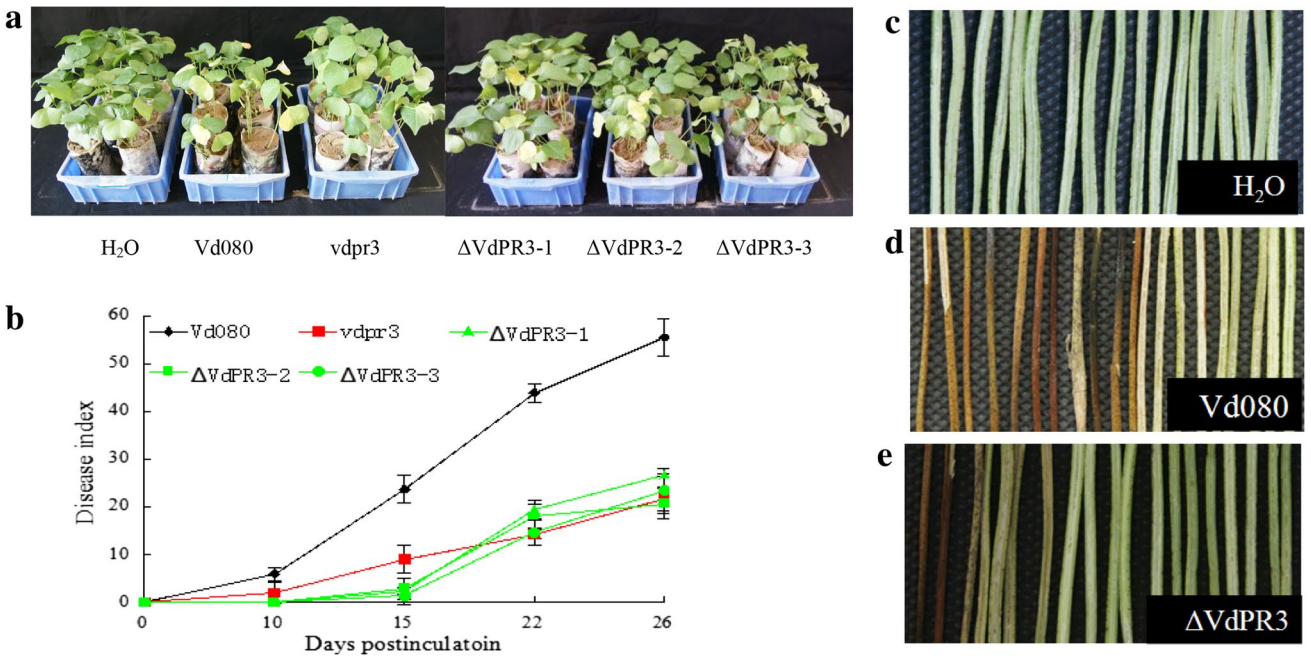

Fig. 6 Pathogenicity analysis of deletion mutants and Vd080. **a** Cotton plants at 26 days post-inoculation with Vd080, vdpr3, or ΔVdPR3. **b** Disease symptom progress caused by *VdPR3* knockout mutants and Vd080. **c** Symptomatic stems of cotton plants inoculated with H_2O. **d** Symptomatic stems of cotton plants inoculated with Vd080. **e** Symptomatic stems of cotton plants inoculated with ΔVdPR3

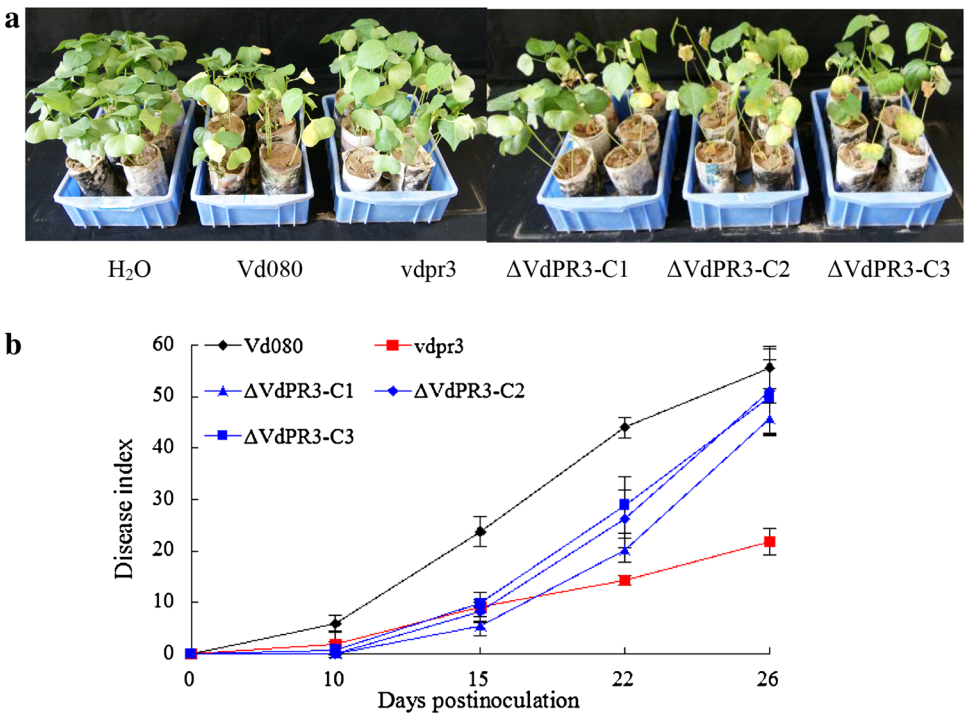

Fig. 7 Pathogenicity analysis of complementary mutants. **a** Symptomatic cotton plants by 26 days post-inoculation with Vd080, vdpr3, or complementary mutants. **b** Progression of the disease caused by *VdPR3* complementary mutants and Vd080

to 26.71 ± 0.3 (Fig. 6a, b). *Verticillium dahliae* causes vascular wilt in host plants, and systemic infection in cotton is also evidenced by browning of vascular tissue. There was no browning phenomenon in the water control (Fig. 6c), but most cotton plants inoculated with Vd080 exhibited browning stems and vascular wilt symptoms, with a discoloration rate of 70 % (Fig. 6d). In contrast, the browning phenomenon was only observed in the stems of a few

ΔVdPR3-infected plants, with a discoloration rate of 37 % (Fig. 6e). These results provide strong evidence that *VdPR3* is an important pathogenicity-related gene required for successful and efficient colonization in cotton plants and that it confers pathogenicity on *V. dahliae*.

To further confirm the virulence function of *VdPR3*, a functional *VdPR3* copy was reintroduced into the vdpr3 mutant to restore its virulence. At only seven dpi, complemented strains showed visual stunting symptoms synchronized with Vd080. At 26 dpi, the infectivity of complementary mutants was recovered and most of the cotton plants appeared to be completely wilted. DI values in the three complementary mutants (ΔVdPR3-C1, ΔVdPR3-C2, and ΔVdPR3-C3) ($P < 0.01$) were remarkably recovered, ranging from 45.71 ± 3.0 to 51.03 ± 8.2 and similar to the wild-type value of 55.62 ± 4.0 ($P < 0.01$) (Fig. 7a, b). This result demonstrates that *VdPR3* contributes to the ability of *V. dahliae* to infect cotton plants.

Discussion

In this study, we uncovered evidence that *VdPR3* is required for cotton infection by *V. dahliae* and is responsible for microsclerotium development. Mutant libraries show great potential for large-scale genome-wide functional analysis of most fungi (Jeon et al. 2007; Hennessy and Doohan 2013; Bourras et al. 2012), as has been the case with *V. dahliae* (Gao et al. 2010). The vdpr3 mutant, with stable cultural characteristics and relatively low pathogenicity, was obtained from an ATMT mutant library of the highly virulent isolate Vd080. The public availability of the genome sequence of *V. dahliae* shortened the amount of time required to identify the T-DNA insertion locus based on detailed genetic blueprints and annotation (Klosterman et al. 2011). According to the results of TAIL-PCR, the flanking sequence of T-DNA showed high identity with VDAG_09942 (VdLs.17). The full-length sequence of *VdPR3* consisting of two exons and one intron was 762 bp long. No other homologous genes were found in the non-redundant protein sequence database. *VdPR3* thus appears to be a species-specific gene of *V. dahliae* with unknown function.

Although microsclerotium development is not always coupled with virulence (Klimes and Dobinson 2006; Tzima et al. 2010), some studies have uncovered evidence that a decrease in microsclerotia and pigmentation reduces survival and pathogenicity of *V. dahliae* isolates (Hawke and Lazarovits 1994; Coley-Smith and Cooke 1971). Germination of microsclerotia is the first step in host invasion and initiation of wilt disease. A total of 1,654 genes showing differential expression have been identified by analysis of whole genome-wide expression profiles of germinating microsclerotia in *V. dahliae* (Hu et al. 2014). To clarify the molecular process contributing to microsclerotium biogenesis and melanin synthesis in *V. dahliae*, an RNA-sequencing and microarray approach was used in another study to screen over 200 differentially expressed genes, including tetrahydroxynaphthalene reductase, scytalone dehydratase, and melanin biosynthetic gene clusters (Duressa et al. 2013). Knockout mutants of *VGB* or *VdGARP1* showed both reduced virulence and decreased microsclerotium production (Tzima et al. 2012; Gao et al. 2010). In our study, the ΔVdPR3 mutant-disrupted VdPR3 in *V. dahliae*, resulting in severely impaired virulence on cotton, a 90 % reduction accompanied by a 6-day postponement of symptoms (Fig. 6b). In addition, ΔVdPR3 could not produce microsclerotia (Figs. 4a, 5a). Consistent with these observations, microsclerotia of *V. dahliae* have always been considered important targets for Verticillium disease control (Debode et al. 2007). Furthermore, *VdPR3* deletion mutants were only weakly invasive with low dispersive ability in cotton, and less stem discoloration was observed in cotton plants inoculated with ΔVdPR3 (Fig. 6d, e).

In general, the cell wall is the first and most important barrier against harmful invasive microorganisms in plants. Plant pathogenic fungi, however, require cell wall-degrading enzymes (CWDEs) for host penetration and successful infection. The soil-borne pathogen *V. dahliae* causes vascular wilt disease, with the xylem serving as a battleground for plant hosts and this fungal pathogen. Xylem infection causes drastic metabolic changes in xylem parenchyma cells located adjacent to infected vessels (Koste and Thomma 2013). To facilitate infection or gain nutrition, fungal pathogens produce a variety of carbohydrate-active enzymes (CAZymes) that degrade plant polysaccharide materials. In general, biotrophic fungi tend to have fewer CAZymes than do necrotrophic and hemibiotrophic fungi (Zhao et al. 2013). For fungal pathogens, localized degradation of cell walls is necessary to access plant cytoplasm and spread across host tissues. In several plant pathogenic fungi, CWDEs such as pectinases and xylanases have been demonstrated to be related to pathogenicity or virulence (Douaiher et al. 2007; Ferrari et al. 2008; Kikot et al. 2009). Although cellulases of some glycoside hydrolase families in fungi are not known to have cellulose-degrading ability, pectinases and cellulases of *V. dahliae* are critical for symptom induction and pathogenesis (Pegg and Brady 2002). These enzymes may be necessary during penetration of plant roots to gain access to xylem and to breach plant defense structures released into xylem vessels in response to infection; finally, at the end of colonization, they may be needed to produce large numbers of survival structures in the plant tissue (Clérivet et al. 2000). Compared with wild-type strain Vd080, ΔVdPR3 significantly reduced the ability to degrade cellulose. The complementary mutant

ΔVdPR3-C recovered the cellulase activity. This result supports the hypothesis that *VdPR3* is a critical CWDE of *V. dahliae*. This multi-faceted gene is therefore required for microsclerotium accumulation and is involved in the pathogenesis of *V. dahliae*. The pathway associated with *VdPR3* has not been studied. Further research is necessary to elucidate the *VdPR3* signaling mechanism in *V. dahliae* and confirm its role on the interaction between cotton and *V. dahliae*, especially in the penetrating, spreading, and colonizing stages.

Acknowledgments The authors wish to thank National Science Foundation of China (No. 31201466) and the National High-tech R and D Program of China (863 Program) (No. 2013AA102601) for the financial support.

Conflict of interest We declared that no conflict of interest exists.

References

Altschul SF, Madden TL, Schäffer AA, Zhang J, Zhang Z, Miller W (1997) Gapped BLAST and PSI-BLAST: a new generation of protein database search programs. Nucleic Acids Res 25:3389–3402

Bourras S, Meyer M, Grandaubert J, Lapalu N, Fudal I, Linglin J (2012) Incidence of genome structure, DNA asymmetry, and cell physiology on T-DNA integration in chromosomes of the phytopathogenic fungus Leptosphaeria maculans. G3 Genes Genom Genet 2:891–904

Clérivet A, Déon V, Alami I, Lopez F, Geiger JP (2000) Tyloses and gels associated with cellulose accumulation in vessels are responses of plane tree seedlings (*Platanus* × *acerifolia*) to the vascular fungus *Ceratocystis fimbriata* f. sp platani. Trees 15:25–31

Coley-Smith JR (1971) Survival and germination of fungal sclerotia. Annu Rev Phytopathol 9:65–92

Debode J, Maeyer KD, Perneel M, Pannecoucque J, Backer GD (2007) Biosurfactants are involved in the biological control of Verticillium microsclerotia by *Pseudomonas* spp. J Appl Microbiol 103:1184–1196

Douaiher MN, Nowak E, Durand R, Halama P (2007) Correlative analysis of Mycosphaerella graminicola pathogenicity and cell wall-degrading enzymes produced in vitro: the importance of xylanase and polygalacturonase. Plant Pathol 56:79–86

Duressa D, Anchieta A, Chen D, Klimes A, Garcia-Pedrajas MD, Dobinson KF (2013) RNA-seq analyses of gene expression in the microsclerotia of *Verticillium dahliae*. BMC Genom 14:607

Ferrari S, Galletti R, Pontiggia D, Manfredini C, Lionetti V, Bellincampi D (2008) Transgenic expression of a fungal endo-polygalacturonase increases plant resistance to pathogens and reduces auxin sensitivity. Plant Physiol 146:669–681

Fradin EF (2006) Physiology and molecular aspects of Verticillium wilt diseases caused by *V. dahliae* and *V. albo-atrum*. Mol Plant Pathol 7:71–86

Gao F, Zhou BJ, Li GY, Jia PS, Li H, Zhao YL (2010) A glutamic acid-rich protein identified in *Verticillium dahliae* from an insertional mutagenesis affects microsclerotial formation and pathogenicity. PLoS One 5:e15319

Hawke MA (1994) Production and manipulation of individual microsclerotia of *Verticillium dahliae* for use in studies of survival. Phytopathology 84:883–890

Hennessy RC, Doohan F (2013) Generating phenotypic diversity in a fungal biocatalyst to investigate alcohol stress tolerance encountered during microbial cellulosic biofuel production. PLoS One 8:e77501

Hu D, Wang C, Tao F, Cui Q, Xu X, Shang W (2014) Whole genome wide expression profiles on germination of *Verticillium dahliae* microsclerotia. PLoS One 9:e100046

James C (2002) Global review of commercialized transgenic crops: 2001 feature: Bt cotton 26. ISAAA

Jeon J, Park SY, Chi MH, Choi J, Park J, Rho HS (2007) Genome-wide functional analysis of pathogenicity genes in the rice blast fungus. Nat Genet 39:561–565

Khang CH, Park SY, Lee YH (2005) A dual selection based, targeted gene replacement tool for Magnaporthe grisea and *Fusarium oxysporum*. Fungal Genet Biol 42:483–492

Kikot GE, Hours RA (2009) Contribution of cell wall degrading enzymes to pathogenesis of *Fusarium graminearum*: a review. J Basic Microb 49:231–241

Klimes A (2006) A hydrophobin gene, VDH1, is involved in microsclerotial development and spore viability in the plant pathogen *Verticillium dahliae*. Fungal Genet Biol 43:283–294

Klimes A, Amyotte SG, Grant S, Kang S (2008) Microsclerotia development in *Verticillium dahliae*: regulation and differential expression of the hydrophobin gene VDH1. Fungal Genet Biol 45:1525–1532

Klosterman SJ, Atallah ZK, Vallad GE (2009) Diversity, pathogenicity, and management of *Verticillium* species. Annu Rev Phytopathol 47:39–62

Klosterman SJ, Subbarao KV, Kang S, Veronese P, Gold SE, Thomma BP (2011) Comparative genomics yields insights into niche adaptation of plant vascular wilt pathogens. PLoS Pathog 7:e1002137

Levin AG (2003) Vegetative compatibility and pathogenicity of *Verticillium dahliae* Kleb. isolates from olive in Israel. J Phytopathol 151:451–455

Liu YG (1995) Thermal asymmetric interlaced PCR: automatable amplification and sequencing of insert end fragments from P1 and YAC clones for chromosome walking. Genomics 25:674–681

Liu SY, Chen JY, Wang JL, Li L, Xiao HL, Adam SM (2013) Molecular characterization and functional analysis of a specific secreted protein from highly virulent defoliating *Verticillium dahliae*. Gene 529:307–316

Liu YJ, Li ZF, Feng ZL, Zhao LH, Zhou FF, Shi YQ (2015) Phenotypic analysis of low pathogenic *Verticillium dahliae* mutants on cotton and cloning of pathogenicity related genes. Acta Phytopathol Sinica. doi:10.13926/j.cnki.apps.2015.02.014

Maruthachalam K, Klosterman SJ, Kang S, Hayes RJ (2011) Identification of pathogenicity-related genes in the vascular wilt fungus *Verticillium dahliae* by *Agrobacterium tumefaciens*-mediated T-DNA insertional mutagenesis. Mol Biotechnol 49:209–221

Mullins ED (2001) Transformation: a tool for studying fungal pathogens of plants. Cell Mol Life S 58:2043–2052

Neumann MJ (2003) Sequence tag analysis of gene expression during pathogenic growth and microsclerotia development in the vascular wilt pathogen *Verticillium dahliae*. Fungal Genet Biol 38:54–62

Pegg GF (2002) Verticillium wilts. CABI

Rauyaree P, Ospina-Giraldo MD, Kang S, Bhat RG, Subbarao KV, Grant SJ (2005) Mutations in VMK1, a mitogen-activated protein kinase gene, affect microsclerotia formation and pathogenicity in *Verticillium dahliae*. Curr Genet 48:109–116

Sambrook J, Russell DW (2001) Molecular cloning: a laboratory manual (3-volume set), vol 999. Cold spring harbor laboratory press, New York

Santhanam P, van Esse HP, Albert I, Faino L, Nürnberger T (2013) Evidence for functional diversification within a fungal NEP1-like protein family. Mol Plant Microbe Interact 26:278–286

Schnathorst WC (1981) Life cycle and epidemiology of Verticillium. Fungal wilt Dis Plants: 81–111

Tzima AK, Paplomatas EJ, Rauyaree P (2010) Roles of the catalytic subunit of cAMP-dependent protein kinase A in virulence and development of the soilborne plant pathogen *Verticillium dahliae*. Fungal Genet Biol 47:406–415

Tzima AK, Paplomatas EJ, Rauyaree P, Ospina-Giraldo MD (2011) VdSNF1, the sucrose nonfermenting protein kinase gene of *Verticillium dahliae*, is required for virulence and expression of genes involved in cell-wall degradation. Mol Plant Microbe Interact 24:129–142

Tzima AK, Paplomatas EJ, Tsitsigiannis DI (2012) The G protein β subunit controls virulence and multiple growth-and development-related traits in *Verticillium dahliae*. Fungal Genet Biol 49:271–283

Vallad GE (2008) Colonization of resistant and susceptible lettuce cultivars by a green fluorescent protein-tagged isolate of *Verticillium dahliae*. Phytopathology 98:871–885

Wang JY, Cai Y, Gou JY, Mao YB, Xu YH, Jiang WH (2004) VdNEP, an elicitor from *Verticillium dahliae*, induces cotton plant wilting. Appl Environ Microb 70:4989–4995

Xia ZJ, Achar PN (1998) Vegetative compatibility groupings of *Verticillium dahliae* from cotton in mainland China. Eur J Plant Pathol 104:871–876

Yadeta KA (2013) The xylem as battleground for plant hosts and vascular wilt pathogens. Front Plant Sci 4

Yu JH, Hamari Z, Han KH, Seo JA, Reyes-Domínguez Y (2004) Double-joint PCR: a PCR-based molecular tool for gene manipulations in filamentous fungi. Fungal Genet Biol 41:973–981

Zhao Z, Liu H, Wang C (2013) Comparative analysis of fungal genomes reveals different plant cell wall degrading capacity in fungi. BMC Genom 14:274

Zhou Z, Li G, Lin C (2009) Conidiophore stalk-less1 encodes a putative zinc-finger protein involved in the early stage of conidiation and mycelial infection in *Magnaporthe oryzae*. Mol Plant Microbe Interact 22:402–410

Zhou BJ, Jia PS, Gao F (2012a) Molecular characterization and functional analysis of a necrosis-and ethylene-inducing, protein-encoding gene family from *Verticillium dahliae*. Mol Plant Microbe Interact 25:964–975

Zhou FF, Li ZF, F ZL (2012b) Construction of T-DNA inserted transformation library of *Verticillium dahliae* on cotton and analysis of mutative traits. Acta Agriculturae Boreali-Occidentalis Sinica 08:19–25

Zhu HQ, Feng ZL, Li ZF, Shi YQ, Zhao LH (2013) Characterization of two fungal isolates from cotton and evaluation of their potential for biocontrol of Verticillium wilt of cotton. J Phytopathol 161:70–77